

Fig. 7.7

Density plot of the imaginary part of the dynamical spin susceptibility calculated from (7.212), showing the band of width  $2k_F$  that spreads up to higher energies. Excitations on the left side of the band correspond to low-momentum-transfer excitations of electrons from just beneath the Fermi surface to just above the Fermi surface. Excitations on the right-hand side of the band correspond to high-momentum-transfer processes, right across the Fermi surface.

where the imaginary part determines the dissipative part of the magnetic response. The dissipation arises because an applied magnetic field generates a cloud of electron–hole pairs which carry away the energy. If we use the Cauchy–Dirac relation  $1/(x + i\delta) = P(1/x) - i\pi\delta(x)$  in (7.202), we obtain

$$\chi''(\mathbf{q}, \nu) = 2\mu_B^2 \int_{\mathbf{k}} \pi \delta[\nu - (\epsilon_{\mathbf{k}+\mathbf{q}} - \epsilon_{\mathbf{k}})] (f_{\mathbf{k}} - f_{\mathbf{k}+\mathbf{q}}). \quad (7.206)$$

This quantity defines the density of states of particle–hole excitations. The excitation energy of a particle–hole pair is given by

$$\epsilon_{\mathbf{k}+\mathbf{q}} - \epsilon_{\mathbf{k}} = \frac{q^2}{2m} + \frac{qk}{m} \cos \theta,$$

where  $\theta$  is the angle between  $\mathbf{k}$  and  $\mathbf{q}$ . This quantity is largest when  $\theta = 0$ ,  $k = k_F$ , and smallest when  $\theta = \pi$ ,  $k = k_F$ , so that

$$\frac{q^2}{2m} + \frac{qk_F}{m} > \nu > \frac{q^2}{2m} - \frac{qk_F}{m}$$

defines a band of allowed wavevectors where the particle–hole density of states is finite, as shown in Figure 7.7. Outside this region,  $\chi_0(\mathbf{q}, \nu)$  is purely real.

## 7.6.2 Derivation of the Lindhard function

The dynamical spin susceptibility

$$\chi(\mathbf{q}, \nu) = 2\mu_B^2 \int_{\mathbf{k}} \frac{f_{\mathbf{k}} - f_{\mathbf{k}+\mathbf{q}}}{(\epsilon_{\mathbf{k}+\mathbf{q}} - \epsilon_{\mathbf{k}} - \nu)} \quad (7.207)$$

can be rewritten as

$$\chi(\mathbf{q}, \nu) = 2\mu_B^2 \int_{\mathbf{k}} f_{\mathbf{k}} \left[ \frac{1}{(\epsilon_{\mathbf{k}+\mathbf{q}} - \epsilon_{\mathbf{k}} - \nu)} + \frac{1}{(\epsilon_{\mathbf{k}-\mathbf{q}} - \epsilon_{\mathbf{k}} + \nu)} \right]. \quad (7.208)$$

Written out explicitly, this is

$$\chi(\mathbf{q}, \nu) = 2\mu_B^2 \int_0^{k_F} \frac{k^2 dk}{2\pi^2} \int_{-1}^1 \frac{d \cos \theta}{2} \left[ \frac{1}{(\epsilon_{\mathbf{k}+\mathbf{q}} - \epsilon_{\mathbf{k}} - \nu)} + ((\nu, \mathbf{q}) \rightarrow -(\nu, \mathbf{q})) \right].$$

By replacing  $\epsilon_{\mathbf{k}} \rightarrow \frac{k^2}{2m} - \mu$  and rescaling  $x = k/k_F$ ,  $\tilde{q} = q/(2k_F)$ , and  $\tilde{\nu} = \nu/(4\epsilon_F)$ , we obtain  $\chi(\mathbf{q}, \nu) = 2\mu_B^2 N(0) \mathcal{F}(\tilde{q}, \tilde{\nu})$ , where

$$\mathcal{F}(\tilde{q}, \tilde{\nu}) = \frac{1}{4\tilde{q}} \int_0^1 x^2 dx \int_{-1}^1 dc \left[ \frac{1}{xc + \tilde{q} - \frac{\tilde{\nu}}{\tilde{q}}} + (\nu \rightarrow -\nu) \right] \quad (7.209)$$

is the Lindhard function. Carrying out the integral over angle, we obtain

$$\begin{aligned} \mathcal{F}(\tilde{q}, \tilde{\nu}) &= \frac{1}{4\tilde{q}} \int_0^1 x dx \left( \ln \left[ \frac{\tilde{q} - \frac{\tilde{\nu}}{\tilde{q}} + x}{\tilde{q} - \frac{\tilde{\nu}}{\tilde{q}} - x} \right] + (\tilde{\nu} \rightarrow -\tilde{\nu}) \right) & \chi(\tilde{q}, \nu) = 2N(0) F(\tilde{q}, \tilde{\nu}) \\ &= \frac{1}{8\tilde{q}} \left( \left[ 1 - \left( \tilde{q} - \frac{\tilde{\nu}}{\tilde{q}} \right)^2 \right] \ln \left[ \frac{\tilde{q} - \frac{\tilde{\nu}}{\tilde{q}} + 1}{\tilde{q} - \frac{\tilde{\nu}}{\tilde{q}} - 1} \right] + (\tilde{\nu} \rightarrow -\tilde{\nu}) \right) + \frac{1}{2}. & \tilde{q} = q/2k_F \quad \tilde{\nu} = \nu/4\epsilon_F \end{aligned} \quad (7.210)$$

Its static limit,  $F(\tilde{q}) = \mathcal{F}(\tilde{q}, \tilde{\nu} = 0)$ ,

$$F(\tilde{q}) = \frac{1}{4\tilde{q}} \left( \left[ 1 - \tilde{q}^2 \right] \ln \left| \frac{\tilde{q} + 1}{\tilde{q} - 1} \right| \right) + \frac{1}{2}, \quad (7.211)$$

has the properties that  $F(0) = 1$  and  $dF/dx$  is singular at  $x = 1$ , as shown in Figure 7.6.

The imaginary part of  $\chi(\mathbf{q}, \nu + i\delta)$  is given by

$$\chi''(\mathbf{q}, \nu) = 2\mu_B^2 N(0) \times \frac{\pi}{8\tilde{q}} \left\{ \left( 1 - \left[ \tilde{q} - \frac{\tilde{\nu}}{\tilde{q}} \right]^2 \right) \theta \left[ 1 - \left[ \tilde{q} - \frac{\tilde{\nu}}{\tilde{q}} \right]^2 \right] - (\nu \rightarrow -\nu) \right\}, \quad (7.212)$$

and is plotted in Figure 7.7.

## 7.7 The RPA (large- $N$ ) electron gas

Although the Feynman diagram approach gives us a way to generate all perturbative corrections, we still need a way to select the physically important diagrams. In general, as we have seen from the previous examples, it is important to re-sum particular classes of diagrams to obtain a physical result. What principles can be used to select classes of diagrams?

Frequently, however, there is no obvious choice of small parameter, in which case one needs an alternative strategy. For example, in the electron gas we could select diagrams according to the power of  $r_s$  entering the diagram. This would give us a high-density expansion of the properties – but what if we would like to examine a low-density electron gas in a controlled way?

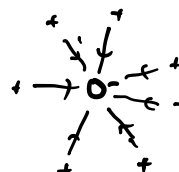
One way to select Feynman diagrams in a system with no natural small parameter is to take the so-called *large- $N$*  limit. This involves generalizing some internal degree of freedom so that it has  $N$  components. Examples include:

# LECTURE 14. RPA Continued.

$$V_{\text{eff}} = - \text{---} = - \left[ \text{---} + \text{---} + \text{---} + \dots \right]$$

$$= \frac{1}{N} \frac{V_0}{1 + V_0 \chi_0(q)} \quad \left\{ \begin{array}{l} V_0 = \tilde{e}^2/q^2 \\ \chi_0 = N(0) F(q/2k_F, \nu/4E_F) \end{array} \right. \quad \tilde{e}^2 = 2e^2/\epsilon_0$$

$$V_{\text{eff}} = \frac{e^2}{\epsilon_0 q^2 \epsilon(q)} \rightarrow \frac{e^2}{\epsilon_0 (q^2 + \kappa^2)}$$



$$V(r) = \frac{e^2}{4\pi\epsilon_0} \frac{1}{r} - \underbrace{\frac{e^2}{4\pi\epsilon_0 r} (1 - e^{-\kappa r})}_{\text{screening charge}}$$

$$\kappa^2 = \tilde{e}^2 N(0)$$

$$\epsilon(q) = 1 + V_0 \chi(q) = 1 + \left( \frac{2e^2 N(0)}{\epsilon_0} \right) \frac{1}{q^2} F(\tilde{q}, \tilde{\nu})$$

$$\epsilon(q) = 1 + \frac{1}{\pi k_F a_B} \left( \frac{F}{\tilde{q}^2} \right)$$

$$Z = \int \mathcal{D}[\phi] \mathcal{D}[\bar{\psi}, \psi] \exp \left[ - \int d^3x d\tau \mathcal{L} \right]$$

$$\mathcal{L} = \bar{\psi} \left[ \partial_\tau - \frac{\nabla^2}{2} - \mu - \phi - v_e \right] \psi - \frac{(\nabla \phi)^2}{e^2} N$$

$$Z = Z_e^0 \int \mathcal{D}[\phi] e^{-S_{\text{eff}}[\phi, v_e]}$$

$$S_{\text{eff}} = \frac{N}{2} \sum_q \left[ |\phi_q|^2 \left( -\frac{q^2}{e^2} \right) - |\phi_q + v_q|^2 \chi_0(q) \right]$$

$$= \frac{N}{2} \sum_q |\phi_q|^2 \underbrace{\left( -\frac{q^2}{e^2} - \chi_0(q) \right)}_{-D^{-1}} - \frac{N}{2} \sum_q \left[ \bar{\phi}_q v_q + \bar{v}_q \phi_q \right] \chi_0(q) - \frac{N}{2} \sum_q |v_q|^2 \chi_0(q)$$

$$Z = Z_e^0 e^{-S_{\text{EM}}}$$

$$S_{\text{EM}} = \frac{1}{2} \sum_q \ln \left[ -\frac{q^2}{e^2} - \chi_0(q) \right] + \frac{N}{2} \left\{ \bar{v}_q \left[ \frac{\chi_0(q)}{\frac{q^2}{e^2} + \chi_0(q)} - \chi_0(q) \right] v_q \right. \\ \left. - \frac{|v_q|^2}{2} \chi_0(q) N \right\}$$

$$= \frac{1}{2} \sum_q \ln \left[ -\frac{q^2}{e^2} - \chi_0(q) \right] - \frac{N}{2} \sum_q |v_q|^2 \tilde{\chi}(q)$$

$$\frac{\chi^2}{\frac{q^2}{e^2} + \chi} = \left( \frac{\frac{e^2 q^2 \chi^2}{q^2}}{1 + \frac{e^2}{q^2} \chi} \right)$$

$$\tilde{\chi}(q) = \frac{\chi_0(q)}{1 + \frac{e^2}{q^2} \chi_0(q)}$$

$$\frac{\chi}{1 + \frac{e^2}{q^2} \chi} - \chi = \frac{-\chi}{1 + \frac{e^2}{q^2} \chi}$$

$$\left[ \text{O} + \text{O} \text{---} \text{O} + \text{O} \text{---} \text{O} \text{---} \text{O} + \dots \right]$$

$$-\frac{\delta S}{\delta V_q} = \langle \delta g_i \rangle = N \tilde{\chi}(q) V(q)$$

$$= \text{Diagram 1} + \text{Diagram 2} + \text{Diagram 3}$$

$$\Delta F = \frac{1}{2} \sum_{\mathbf{k}} \ln(1 + \chi(\mathbf{q}, \frac{\tilde{\epsilon}^2}{q^2}) e^{z0^+})$$

$$= \frac{1}{2} \sum_{\mathbf{k}} \oint \frac{dz}{2\pi i} (n(z) + \frac{1}{2}) \# = -\frac{1}{2} \sum_{\mathbf{k}} \int \frac{d\omega}{\pi} \ln \frac{\ln(1 + \frac{e^2 \chi(\mathbf{q}, \omega - i\delta)}{q^2})}{(\frac{1}{2} + n(\omega))}$$

$$\text{Diagram 1} = \text{Diagram 2} = -\frac{V}{2} \int \frac{d^3 q}{(2\pi)^3} \int \frac{d\omega}{\pi} (\frac{1}{2} + n(\omega)) \ln \left[ 1 + \frac{e^2 \chi_0}{q^2} \right]$$

$$\frac{F}{V} = -NT \int_{\mathbf{k}} \ln(1 + e^{-\beta E_{\mathbf{k}}}) + \frac{\Delta F}{V}$$

where the dimensionless coupling constant

$$\lambda = \frac{\tilde{e}^2 N(0)}{(2k_F)^2} = \frac{1}{\pi k_F} \frac{e^2 m}{4\pi \epsilon_0 \hbar^2} = \frac{1}{\pi k_F a_B} = \left(\frac{\alpha}{\pi}\right) r_s. \quad (7.230)$$

Here  $a_B$  is the Bohr radius  $\alpha = \left(\frac{4}{9\pi}\right)^{1/3} \approx 0.521$  and  $r_s = (\alpha k_F a_B)^{-1}$  is the dimensionless electron separation (7.112). Notice that the accuracy of the large- $N$  expansion places no restriction on the size of the coupling constant  $\lambda$ , which may take any value in the large- $N$  limit. Summarizing,

$$\epsilon_{RPA}(\mathbf{q}, \omega) = 1 + \frac{1}{\pi k_F a_B} \left( \frac{\mathcal{F}(\tilde{q}, \tilde{\nu})}{\tilde{q}^2} \right). \quad (7.231)$$

dielectric constant of the RPA electron gas

## 7.7.2 Screening and plasma oscillations

At zero frequency and low momentum,  $\mathcal{F} \rightarrow 1$ , so the dielectric constant diverges:

$$\epsilon = \lim_{q \rightarrow 0} \epsilon(\mathbf{q}, \nu = 0) \rightarrow \infty.$$

Is this a failure of our theory?

In fact, no. The divergence of the uniform, static dielectric constant is a quintessential property of a metal. Since  $\epsilon = \infty$ , no static electric fields penetrate a metal. Moreover, the electron charge is completely screened. At small  $q$ , the effective interaction is

$$V_{eff}(\mathbf{q}, \nu) = \frac{1}{N} \frac{\tilde{e}^2}{q^2 + \kappa^2} \equiv \frac{e^2}{\epsilon_0(q^2 + \kappa^2)} \quad (N = 2), \quad (7.232)$$

where

$$\kappa = \sqrt{\tilde{e}^2 N(0)} = \sqrt{2e^2 N(0)/\epsilon_0} \quad (N = 2) \quad (7.233)$$

can be identified as an inverse screening length.  $\kappa^{-1}$  is the Thomas–Fermi screening length of a classical charge plasma. You can think of

$$V_{screening}(q) = \frac{e^2}{\epsilon_0(q^2 + \kappa^2)} - \frac{e^2}{\epsilon_0 q^2}$$

as the screening potential. If we Fourier transform this potential, we obtain  $V_{screen}(r) = eQ(r)/(4\pi r)$  where  $Q(r) = -(1 - e^{-\kappa r})$  is the screening charge. We can see that the electron charge is fully screened at infinity, since  $Q(\infty) = -1$ . Note, however, that there is still a weak singularity in the susceptibility when  $q \sim 2k_F$ ,  $\chi_0(q \sim 2k_F, 0) \sim (q - 2k_F) \ln(q - 2k_F)$ ; Fourier transformed, this gives rise to a long-range *oscillatory* component to the interaction between the particles, of the form

$$V_{eff}(r) \propto \frac{\cos 2k_F r}{r^3} \quad (7.234)$$

(see Example 17.1). This long-range oscillatory interaction is associated with Friedel oscillations.



A second and related consequence of the screening is the emergence of collective plasma oscillations. In the opposite limit of finite frequency but low momentum, we may approximate  $\chi_0$  by expanding it in momentum, as follows:

$$\chi_0(\mathbf{q}, \nu) = \int_{\mathbf{k}} \frac{f_{\mathbf{k}+\mathbf{q}} - f_{\mathbf{k}}}{\nu - (\epsilon_{\mathbf{k}+\mathbf{q}} - \epsilon_{\mathbf{k}})} \approx \int_{\mathbf{k}} \frac{(\mathbf{q} \cdot \mathbf{v}_{\mathbf{k}})}{\nu - (\mathbf{q} \cdot \mathbf{v}_{\mathbf{k}})} \left( \frac{df(\epsilon)}{d\epsilon} \right), \quad (7.235)$$

where  $\mathbf{v}_{\mathbf{k}} = \nabla_{\mathbf{k}} \epsilon_{\mathbf{k}}$  is the group velocity. Expanding this to leading order in momentum gives

$$\chi_0(\mathbf{q}, \nu) = - \int_{\mathbf{k}} \frac{(\mathbf{q} \cdot \mathbf{v}_{\mathbf{k}})^2}{\nu^2} \left( - \frac{df(\epsilon)}{d\epsilon} \right) = - \frac{N(0)v_F^2}{3} \left( \frac{q^2}{\nu^2} \right) = - \left( \frac{\tilde{n}}{m} \right) \left( \frac{q^2}{\nu^2} \right), \quad (7.236)$$

where  $\tilde{n} = n/N$  is the density of electrons per spin, so that the RPA dielectric function (7.228) is given by

$$\epsilon_{RPA}(\mathbf{q}, \nu) = 1 + \frac{\tilde{e}^2}{q^2} \chi_0(\mathbf{q}, \omega) = 1 - \frac{\omega_p^2}{\nu^2}, \quad (7.237)$$

where

$$\omega_p^2 = \frac{\tilde{e}^2 \tilde{n}}{m} = \frac{e^2 n}{\epsilon_0 m} \quad (N = 2) \quad (7.238)$$

is the plasma frequency. This zero in the dielectric function at  $\nu = \omega_p$  indicates the presence of collective plasma oscillations in the medium at frequency  $\omega_p$ . At finite  $q$ ,  $\omega_p(q)$  develops a collective mode.

It is instructive to examine the response of the electron gas to a time-dependent change in potential energy,  $-\delta U(x, t)$  (corresponding to a change in energy  $H = - \int \delta U(x, t) \rho(x)$ ), with Fourier transform  $\delta U(q)$ . In a non-interacting electron gas, the induced change in charge is

$$\delta \rho_e(q) = N \chi_0(q) \delta U(q),$$

corresponding to the diagram

$$\delta \rho_e(q) = -i \left[ \text{bubble diagram} \right] \delta U(q). \quad (7.239)$$

In the RPA electron gas, the change in the electron density induced by the applied potential produces its own interaction, and the induced change in charge is given by

$$\begin{aligned} \delta \rho_e(q) &= -i \left[ \text{bubble} + \text{bubble with bubble} + \text{bubble with two bubbles} + \dots \right] \delta U(q) \\ &= N \left[ \chi_0 + \chi_0(-\mathcal{V}\chi_0) + \chi_0(-\mathcal{V}\chi_0)^2 + \dots \right] \delta U(q) \\ &= N \left[ \frac{\chi_0(q)}{1 + \mathcal{V}_q \chi_0(q)} \right] \delta U(q). \end{aligned} \quad (7.240)$$

A second and related consequence of the screening is the emergence of collective of plasma oscillations. In the opposite limit of finite frequency but low momentum, we may approximate  $\chi_0$  by expanding it in momentum, as follows:

$$\chi_0(\mathbf{q}, \nu) = \int_{\mathbf{k}} \frac{f_{\mathbf{k}+\mathbf{q}} - f_{\mathbf{k}}}{\nu - (\epsilon_{\mathbf{k}+\mathbf{q}} - \epsilon_{\mathbf{k}})} \approx \int_{\mathbf{k}} \frac{(\mathbf{q} \cdot \mathbf{v}_{\mathbf{k}})}{\nu - (\mathbf{q} \cdot \mathbf{v}_{\mathbf{k}})} \left( \frac{df(\epsilon)}{d\epsilon} \right), \quad (7.235)$$

where  $\mathbf{v}_{\mathbf{k}} = \nabla_{\mathbf{k}} \epsilon_{\mathbf{k}}$  is the group velocity. Expanding this to leading order in momentum gives

$$\chi_0(\mathbf{q}, \nu) = - \int_{\mathbf{k}} \frac{(\mathbf{q} \cdot \mathbf{v}_{\mathbf{k}})^2}{\nu^2} \left( - \frac{df(\epsilon)}{d\epsilon} \right) = - \frac{N(0)v_F^2}{3} \left( \frac{q^2}{\nu^2} \right) = - \left( \frac{\tilde{n}}{m} \right) \left( \frac{q^2}{\nu^2} \right), \quad (7.236)$$

where  $\tilde{n} = n/N$  is the density of electrons per spin, so that the RPA dielectric function (7.228) is given by

$$\epsilon_{RPA}(\mathbf{q}, \nu) = 1 + \frac{\tilde{e}^2}{q^2} \chi_0(\mathbf{q}, \omega) = 1 - \frac{\omega_p^2}{\nu^2}, \quad (7.237)$$

where


$$\omega_p^2 = \frac{\tilde{e}^2 \tilde{n}}{m} = \frac{e^2 n}{\epsilon_0 m} \quad (N = 2) \quad (7.238)$$

is the plasma frequency. This zero in the dielectric function at  $\nu = \omega_p$  indicates the presence of collective plasma oscillations in the medium at frequency  $\omega_p$ . At finite  $q$ ,  $\omega_p(q)$  develops a collective mode.


It is instructive to examine the response of the electron gas to a time-dependent change in potential energy,  $-\delta U(x, t)$  (corresponding to a change in energy  $H = - \int \delta U(x, t) \rho(x)$ ), with Fourier transform  $\delta U(q)$ . In a non-interacting electron gas, the induced change in charge is

$$\delta \rho_e(q) = N \chi_0(q) \delta U(q),$$

corresponding to the diagram

$$\delta \rho_e(q) = -i \left[ \text{diagram} \right] \delta U(q). \quad (7.239)$$


In the RPA electron gas, the change in the electron density induced by the applied potential produces its own interaction, and the induced change in charge is given by

$$\begin{aligned} \delta \rho_e(q) &= -i \left[ \text{diagram 1} + \text{diagram 2} + \text{diagram 3} + \dots \right] \delta U(q) \\ &= N \left[ \chi_0 + \chi_0(-\mathcal{V}\chi_0) + \chi_0(-\mathcal{V}\chi_0)^2 + \dots \right] \delta U(q) \\ &= N \left[ \frac{\chi_0(q)}{1 + \mathcal{V}_q \chi_0(q)} \right] \delta U(q). \end{aligned} \quad (7.240)$$




A second and related consequence of the screening is the emergence of collective of plasma oscillations. In the opposite limit of finite frequency but low momentum, we may approximate  $\chi_0$  by expanding it in momentum, as follows:

$$\chi_0(\mathbf{q}, \nu) = \int_{\mathbf{k}} \frac{f_{\mathbf{k}+\mathbf{q}} - f_{\mathbf{k}}}{\nu - (\epsilon_{\mathbf{k}+\mathbf{q}} - \epsilon_{\mathbf{k}})} \approx \int_{\mathbf{k}} \frac{(\mathbf{q} \cdot \mathbf{v}_{\mathbf{k}})}{\nu - (\mathbf{q} \cdot \mathbf{v}_{\mathbf{k}})} \left( \frac{df(\epsilon)}{d\epsilon} \right), \quad (7.235)$$

where  $\mathbf{v}_{\mathbf{k}} = \nabla_{\mathbf{k}} \epsilon_{\mathbf{k}}$  is the group velocity. Expanding this to leading order in momentum gives

$$\chi_0(\mathbf{q}, \nu) = - \int_{\mathbf{k}} \frac{(\mathbf{q} \cdot \mathbf{v}_{\mathbf{k}})^2}{\nu^2} \left( - \frac{df(\epsilon)}{d\epsilon} \right) = - \frac{N(0)v_F^2}{3} \left( \frac{q^2}{\nu^2} \right) = - \left( \frac{\tilde{n}}{m} \right) \left( \frac{q^2}{\nu^2} \right), \quad (7.236)$$

where  $\tilde{n} = n/N$  is the density of electrons per spin, so that the RPA dielectric function (7.228) is given by

$$\epsilon_{RPA}(\mathbf{q}, \nu) = 1 + \frac{\tilde{e}^2}{q^2} \chi_0(\mathbf{q}, \omega) = 1 - \frac{\omega_p^2}{\nu^2}, \quad (7.237)$$

where

$$\omega_p^2 = \frac{\tilde{e}^2 \tilde{n}}{m} = \frac{e^2 n}{\epsilon_0 m} \quad (N = 2) \quad (7.238)$$

is the plasma frequency. This zero in the dielectric function at  $\nu = \omega_p$  indicates the presence of collective plasma oscillations in the medium at frequency  $\omega_p$ . At finite  $q$ ,  $\omega_p(q)$  develops a collective mode.

It is instructive to examine the response of the electron gas to a time-dependent change in potential energy,  $-\delta U(x, t)$  (corresponding to a change in energy  $H = - \int \delta U(x, t) \rho(x)$ ), with Fourier transform  $\delta U(q)$ . In a non-interacting electron gas, the induced change in charge is

$$\delta \rho_e(q) = N \chi_0(q) \delta U(q),$$

corresponding to the diagram

$$\delta \rho_e(q) = -i \left[ \text{diagram} \right] \delta U(q). \quad (7.239)$$

In the RPA electron gas, the change in the electron density induced by the applied potential produces its own interaction, and the induced change in charge is given by

$$\begin{aligned} \delta \rho_e(q) &= -i \left[ \text{diagram 1} + \text{diagram 2} + \text{diagram 3} + \dots \right] \delta U(q) \\ &= N \left[ \chi_0 + \chi_0(-\mathcal{V}\chi_0) + \chi_0(-\mathcal{V}\chi_0)^2 + \dots \right] \delta U(q) \\ &= N \left[ \frac{\chi_0(q)}{1 + \mathcal{V}_q \chi_0(q)} \right] \delta U(q). \end{aligned} \quad (7.240)$$

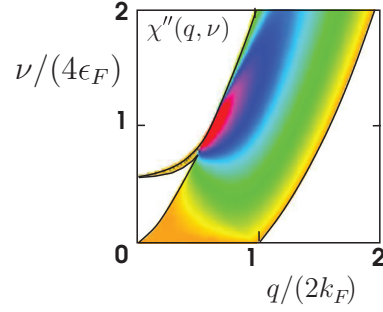


Fig. 7.8

Density plot of the imaginary part of the dynamical charge susceptibility  $\text{Im}[\chi_0(\mathbf{q}, \nu)/\epsilon(\mathbf{q}, \nu)]$  in the presence of the Coulomb interaction, calculated for  $\frac{\alpha r_s}{\pi} = 1$ , ( $r_s \sim 6$ ), using (7.231) and (7.210). Notice the split-off plasmon frequency mode, and how the charge fluctuations have moved up to frequencies above the plasma frequency.

So we see that the dynamical charge susceptibility is renormalized by interactions

$$\chi(q) = N \frac{\chi_0(q)}{\epsilon_{RPA}(q)} = \mathcal{N}(0) \left[ \frac{\mathcal{F}(\tilde{q}, \tilde{\nu})}{1 + \frac{\alpha r_s}{\pi} \mathcal{F}(\tilde{q}, \tilde{\nu})} \right] \quad (\tilde{q} = q/2k_F, \tilde{\nu} = \nu/4\epsilon_F), \quad (7.241)$$

where  $\mathcal{F}(\tilde{q}, \tilde{\nu})$  is given in (7.210) and  $\mathcal{N}(0) = N \times N(0)$  is the total density of states. The imaginary part of the dynamical susceptibility  $\chi(\mathbf{q}, \nu - i\delta)$  defines the spectrum of collective excitations of the RPA electron gas, shown in in Figure 7.8. Notice how the collective plasma mode is split off above the particle–hole continuum.

### Remark

- The appearance of this plasma mode depends on the singular, long-range nature of the Coulomb interaction. It is rather interesting to reflect on what would have happened to the results of this section had we kept the regulating  $\delta$  in the bare interaction  $\mathcal{V}_q$  (7.217) finite. In this case the plasma frequency would be zero, while the dielectric constant would be finite. In other words, the appearance of the plasma mode and the screening of an infinite–range interaction are intimately intertwined. In fact, the plasma mode in the Coulomb gas is an elementary example of a Higgs particle – a finite-mass excitation that results from the screening of a long-range (gauge) interaction. We shall discuss this topic in more depth in Section 11.6.2.

### 7.7.3 The Bardeen–Pines interaction

One of the most famous applications of the RPA approach is the Bardeen–Pines theory [9] for the electron–electron interaction. Whereas the treatment of jellium described so far treats the positive ionic background as a rigid medium, the Bardeen–Pines theory takes account of its finite compressibility. The ions immersed in the electron sea are thousands of times more massive than the surrounding electrons, so their motions are far more sluggish. In particular, the ionic plasma frequency is given by

$$\Omega_P^2 = \frac{(Ze)^2 n_{ion}}{\epsilon_0 M} = \frac{Ze^2 n}{\epsilon_0 M}, \quad (7.242)$$

where  $+Z|e|n_{ion}$  is the charge density of the background ions and  $n_{ion}$  is the corresponding ionic density. The ionic plasma frequency is thousands of times smaller than the electronic plasma frequency. Note that the expression on the right-hand side of (7.242) follows from the requirement of neutrality, which implies that the electron density is  $Z$  times larger than the ionic density,  $|e|n = Z|e|n_{ion} = \rho_+$ . The ionic plasma frequency  $\Omega_P$  sets the characteristic frequency scale for charge fluctuations of the background ionic medium.

The charge polarizability of the combined electron–ion medium now contains two terms: an electron plus an ionic component. In its simplest version, the Bardeen–Pines theory treats the positive ionic background as a uniform plasma. In the RPA (large- $N$ ) approximation, the effective interaction is then

$$V_{eff} = \frac{1}{N} \frac{\mathcal{V}(q)}{1 + \mathcal{V}(q)[\chi_0(q) + \chi_{ion}(q)]} \equiv \frac{1}{N} \frac{\mathcal{V}(q)}{\epsilon(q)}, \quad (7.243)$$

where

$$i[\chi_0(q) + \chi_{ion}(q)]N = \text{Diagram 1} + \text{Diagram 2} \quad (7.244)$$

is the sum of the non-interacting RPA polarizabilities of the electron and ionic plasmas, where the dashed lines represent the ionic propagators. For frequencies relevant for electron–electron interactions, we can approximate the electron component of the polarizability by the low-frequency screening form:

$$\mathcal{V}(q)\chi_0(q) \sim \frac{\kappa^2}{q^2}. \quad (7.245)$$

By contrast, the large ratio of ionic to electron masses guarantees that the ionic part of the polarizability is described by its high-frequency, low- $q$  plasma approximation (7.236), which, for the ions, is

$$\mathcal{V}(q)\chi_{ion}(q) \sim -\frac{\Omega_P^2}{v^2}. \quad (7.246)$$

With these approximations, the combined dielectric constant is then given by

$$\epsilon(q) = 1 + \frac{\kappa^2}{q^2} - \frac{\Omega_P^2}{v^2}. \quad (7.247)$$

Substituting this dielectric constant into (7.243), the effective interaction is then given by

$$V_{eff}(q) = \frac{\tilde{e}^2}{N\epsilon(q)q^2} = \frac{1}{N} \frac{\tilde{e}^2}{(q^2 + \kappa^2 - \Omega_P^2(q^2/v^2))}, \quad (7.248)$$

which we can separate into the form

$$\begin{aligned} V_{eff}(q) &= \frac{\tilde{e}^2}{N} \left[ \frac{1}{q^2 + \kappa^2} \right] \left[ 1 + \frac{\Omega_P^2 \frac{q^2}{v^2}}{q^2 + \kappa^2 - \Omega_P^2 \frac{q^2}{v^2}} \right] \\ &= \frac{\tilde{e}^2}{N} \left[ \frac{1}{q^2 + \kappa^2} \right] \left[ 1 + \frac{\omega_q^2/v^2}{1 - \omega_q^2/v^2} \right], \end{aligned} \quad (7.249)$$

where

$$\omega_q^2 = \Omega_P^2 \frac{q^2}{q^2 + \kappa^2} \quad (7.250)$$

is a renormalized plasma frequency. Replacing  $\tilde{e}^2 \rightarrow (2)(e^2/\epsilon_0)$  and setting  $N = 2$ , we obtain

$$V_{eff}(\mathbf{q}, \nu) = \left[ \frac{e^2}{\epsilon_0(q^2 + \kappa^2)} \right] \left( 1 + \frac{\omega_q^2}{\nu^2 - \omega_q^2} \right). \quad (7.251)$$

Bardeen–Pines interaction

### Remarks

- We see that the electron–electron interaction inside the jellium plasma has split into terms: a repulsive and instantaneous (i.e. frequency-*independent*) screened Coulomb interaction, plus a retarded (i.e. frequency-*dependent*) electron–phonon interaction:

$$V_{eff}(\mathbf{q}, \nu) = \underbrace{\left[ \frac{e^2}{\epsilon_0(q^2 + \kappa^2)} \right]}_{\text{screened Coulomb interaction}} + \overbrace{\left[ \frac{e^2}{\epsilon_0(q^2 + \kappa^2)} \right] \frac{\omega_q^2}{\nu^2 - \omega_q^2}}^{\text{retarded electron–phonon interaction}}. \quad (7.252)$$

It is the retarded attractive interaction produced by the second term that is responsible for Cooper pairing in conventional superconductors (see Exercise 7.7 and [10]).

- The plasma frequency (7.250) is renormalized by the interaction of the positive jellium with the electron sea, to form a dispersing mode with a linear dispersion  $\omega_{\mathbf{q}} = cq$  at low frequencies, where

$$c = \frac{\Omega_P}{\kappa}. \quad (7.253)$$

Now, by (7.233),

$$\kappa^2 = \frac{e^2}{\epsilon_0} N(0) = \frac{e^2}{\epsilon_0} \left( \frac{3n}{2\epsilon_F} \right) = \left( \frac{ne^2}{\epsilon_0 m} \right) \frac{3}{v_F^2} = 3 \frac{\omega_P^2}{v_F^2}, \quad (7.254)$$

where  $\omega_P$  is the electron plasma frequency, so that the sound velocity predicted by the Bardeen–Pines theory is

$$c = \frac{v_F}{\sqrt{3}} \left( \frac{\Omega_P}{\omega_P} \right) = \sqrt{\frac{Z}{3}} \left( \frac{m}{M} \right)^{\frac{1}{2}} v_F, \quad (7.255)$$

a form for the sound velocity first derived by Bohm and Staver [11]. Remarkably, this agrees within a factor of 2 with the experimental sound-velocity for a wide range of metals [9]. In this way, the Bardeen–Pines theory can account for the emergence of longitudinal phonons inside matter as a consequence of the interaction between the plasma modes of the ions and the electron sea.

- The Bardeen–Pines interaction can be used to formulate an effective Hamiltonian for the low-energy physics of jellium, known as the *Bardeen–Pines Hamiltonian*:

$$H_{BP} = \sum_{\mathbf{k}\sigma} \epsilon_{\mathbf{k}} c_{\mathbf{k}\sigma}^{\dagger} c_{\mathbf{k}\sigma} + \frac{1}{2} \sum_{\mathbf{k}, \mathbf{k}'} V_{\text{eff}}(\mathbf{q}, \epsilon_{\mathbf{k}} - \epsilon_{\mathbf{k}'}) c_{\mathbf{k}-\mathbf{q}\sigma}^{\dagger} c_{\mathbf{k}'+\mathbf{q}\sigma'}^{\dagger} c_{\mathbf{k}'\sigma'} c_{\mathbf{k}\sigma}. \quad (7.256)$$

Bardeen–Pines Hamiltonian

The Bardeen–Pines Hamiltonian is the predecessor of the Bardeen–Cooper–Schrieffer (BCS) model, and demonstrates that, while the intrinsic electron–electron interaction is repulsive, “overscreening” by the lattice causes it to develop a retarded attractive component (see Exercise 7.8).

### 7.7.4 Zero-point energy of the RPA electron gas

Let us now examine the linked-cluster expansion of the ground state energy. Without the tadpole insertions, the only non-zero diagrams are then

$$\begin{aligned} \frac{\Delta E}{V} = & \left( \text{diagram 1} + \text{diagram 2} + \text{diagram 3} + \text{diagram 4} + \dots \right) \\ & + \left( \text{diagram 5} + \text{diagram 6} + \dots \right) + \left( \text{diagram 7} + \dots \right) + \dots \end{aligned} \quad (7.257)$$

$\text{diagram 1} \sim \text{diagram 2} \sim \text{diagram 3} \sim \text{diagram 4} \sim \text{diagram 5} \sim \text{diagram 6} \sim \text{diagram 7} \sim \text{diagram 8} \sim \text{diagram 9} \sim \text{diagram 10} \sim \text{diagram 11} \sim \text{diagram 12} \sim \text{diagram 13} \sim \text{diagram 14} \sim \text{diagram 15} \sim \text{diagram 16} \sim \text{diagram 17} \sim \text{diagram 18} \sim \text{diagram 19} \sim \text{diagram 20} \sim \text{diagram 21} \sim \text{diagram 22} \sim \text{diagram 23} \sim \text{diagram 24} \sim \text{diagram 25} \sim \text{diagram 26} \sim \text{diagram 27} \sim \text{diagram 28} \sim \text{diagram 29} \sim \text{diagram 30} \sim \text{diagram 31} \sim \text{diagram 32} \sim \text{diagram 33} \sim \text{diagram 34} \sim \text{diagram 35} \sim \text{diagram 36} \sim \text{diagram 37} \sim \text{diagram 38} \sim \text{diagram 39} \sim \text{diagram 40} \sim \text{diagram 41} \sim \text{diagram 42} \sim \text{diagram 43} \sim \text{diagram 44} \sim \text{diagram 45} \sim \text{diagram 46} \sim \text{diagram 47} \sim \text{diagram 48} \sim \text{diagram 49} \sim \text{diagram 50} \sim \text{diagram 51} \sim \text{diagram 52} \sim \text{diagram 53} \sim \text{diagram 54} \sim \text{diagram 55} \sim \text{diagram 56} \sim \text{diagram 57} \sim \text{diagram 58} \sim \text{diagram 59} \sim \text{diagram 60} \sim \text{diagram 61} \sim \text{diagram 62} \sim \text{diagram 63} \sim \text{diagram 64} \sim \text{diagram 65} \sim \text{diagram 66} \sim \text{diagram 67} \sim \text{diagram 68} \sim \text{diagram 69} \sim \text{diagram 70} \sim \text{diagram 71} \sim \text{diagram 72} \sim \text{diagram 73} \sim \text{diagram 74} \sim \text{diagram 75} \sim \text{diagram 76} \sim \text{diagram 77} \sim \text{diagram 78} \sim \text{diagram 79} \sim \text{diagram 80} \sim \text{diagram 81} \sim \text{diagram 82} \sim \text{diagram 83} \sim \text{diagram 84} \sim \text{diagram 85} \sim \text{diagram 86} \sim \text{diagram 87} \sim \text{diagram 88} \sim \text{diagram 89} \sim \text{diagram 90} \sim \text{diagram 91} \sim \text{diagram 92} \sim \text{diagram 93} \sim \text{diagram 94} \sim \text{diagram 95} \sim \text{diagram 96} \sim \text{diagram 97} \sim \text{diagram 98} \sim \text{diagram 99} \sim \text{diagram 100} \sim \dots$

These diagrams are derived from the zero-point fluctuations in charge density, which modify the ground state energy  $E \rightarrow E_0 + E_{zp}$ . We shall select the leading contribution,

$$\frac{E_{zp}}{V} = \text{diagram 1} + \text{diagram 2} + \text{diagram 3} + \text{diagram 4} + \dots \quad (7.258)$$

$\text{diagram 1} \sim \text{diagram 2} \sim \text{diagram 3} \sim \text{diagram 4} \sim \text{diagram 5} \sim \text{diagram 6} \sim \text{diagram 7} \sim \text{diagram 8} \sim \text{diagram 9} \sim \text{diagram 10} \sim \text{diagram 11} \sim \text{diagram 12} \sim \text{diagram 13} \sim \text{diagram 14} \sim \text{diagram 15} \sim \text{diagram 16} \sim \text{diagram 17} \sim \text{diagram 18} \sim \text{diagram 19} \sim \text{diagram 20} \sim \text{diagram 21} \sim \text{diagram 22} \sim \text{diagram 23} \sim \text{diagram 24} \sim \text{diagram 25} \sim \text{diagram 26} \sim \text{diagram 27} \sim \text{diagram 28} \sim \text{diagram 29} \sim \text{diagram 30} \sim \text{diagram 31} \sim \text{diagram 32} \sim \text{diagram 33} \sim \text{diagram 34} \sim \text{diagram 35} \sim \text{diagram 36} \sim \text{diagram 37} \sim \text{diagram 38} \sim \text{diagram 39} \sim \text{diagram 40} \sim \text{diagram 41} \sim \text{diagram 42} \sim \text{diagram 43} \sim \text{diagram 44} \sim \text{diagram 45} \sim \text{diagram 46} \sim \text{diagram 47} \sim \text{diagram 48} \sim \text{diagram 49} \sim \text{diagram 50} \sim \text{diagram 51} \sim \text{diagram 52} \sim \text{diagram 53} \sim \text{diagram 54} \sim \text{diagram 55} \sim \text{diagram 56} \sim \text{diagram 57} \sim \text{diagram 58} \sim \text{diagram 59} \sim \text{diagram 60} \sim \text{diagram 61} \sim \text{diagram 62} \sim \text{diagram 63} \sim \text{diagram 64} \sim \text{diagram 65} \sim \text{diagram 66} \sim \text{diagram 67} \sim \text{diagram 68} \sim \text{diagram 69} \sim \text{diagram 70} \sim \text{diagram 71} \sim \text{diagram 72} \sim \text{diagram 73} \sim \text{diagram 74} \sim \text{diagram 75} \sim \text{diagram 76} \sim \text{diagram 77} \sim \text{diagram 78} \sim \text{diagram 79} \sim \text{diagram 80} \sim \text{diagram 81} \sim \text{diagram 82} \sim \text{diagram 83} \sim \text{diagram 84} \sim \text{diagram 85} \sim \text{diagram 86} \sim \text{diagram 87} \sim \text{diagram 88} \sim \text{diagram 89} \sim \text{diagram 90} \sim \text{diagram 91} \sim \text{diagram 92} \sim \text{diagram 93} \sim \text{diagram 94} \sim \text{diagram 95} \sim \text{diagram 96} \sim \text{diagram 97} \sim \text{diagram 98} \sim \text{diagram 99} \sim \text{diagram 100} \sim \dots$

The  $n$ th diagram in this series has a symmetry factor  $p = 2n$ , and a contribution  $(-\chi_0(q)\mathcal{V}(q))^n$  associated with the  $n$  polarization bubbles and interaction lines. The energy per unit volume associated with this series of diagrams is thus

$$E_{zp} = i \sum_{n=1}^{\infty} \frac{1}{2n} \int \frac{d^4q}{(2\pi)^4} (-\chi_0(q)\mathcal{V}(q))^n. \quad (7.259)$$

By interchanging the sum and the integral, we see that we obtain a series of the form  $\sum_n \frac{(-x)^n}{n} = -\ln(1+x)$ , so that the zero-point correction to the ground state energy is

$$E_{zp} = -i \frac{1}{2} \int \frac{d^4 q}{(2\pi)^4} \ln[1 + \mathcal{V}_{\mathbf{q}} \chi_0(q)].$$

Now the logarithm has a branch cut just below the real axis for positive frequency, but just above the real axis for negative frequency. If we carry out the frequency integral by completing the contour in the lower half-plane, we can distort the contour integral around the branch cut at positive frequency, to obtain

$$\begin{aligned} E_{zp} &= -\frac{i}{2} \int_{\mathbf{q}} \int_0^{\infty} \frac{d\nu}{2\pi} [\ln[1 + \chi_0(\mathbf{q}, \nu + i\delta)\mathcal{V}_{\mathbf{q}}] - \ln[1 + \chi_0(\mathbf{q}, \nu - i\delta)\mathcal{V}_{\mathbf{q}}]] \\ &= \frac{1}{2} \int_{\mathbf{q}} \int_0^{\infty} \frac{d\nu}{\pi} \arctan \left( \frac{\mathcal{V}_{\mathbf{q}} \chi''(\mathbf{q}, \nu)}{[1 + \mathcal{V}_{\mathbf{q}} \chi'(\mathbf{q}, \nu)]} \right). \end{aligned} \quad (7.260)$$

If we associate a “phase shift”

$$\delta(\mathbf{q}, \nu) = \arctan \left( \frac{\mathcal{V}_{\mathbf{q}} \chi''(\mathbf{q}, \nu)}{[1 + \mathcal{V}_{\mathbf{q}} \chi'(\mathbf{q}, \nu)]} \right), \quad (7.261)$$

then, by integrating by parts, we can also rewrite the zero-point fluctuation energy in the form

$$\Delta E_{zp} = - \int \frac{d^3 q}{(2\pi)^3} \int_0^{\infty} d\nu \Lambda(\nu) \left[ \frac{\nu}{2} \right], \quad (7.262)$$

where

$$\Lambda(\nu) = \frac{1}{\pi} \frac{\partial \delta(\mathbf{q}, \nu)}{\partial \nu}. \quad (7.263)$$

We can interpret  $\Lambda(\omega)$  as the “density of states” of charge fluctuations at an energy  $\nu$ . When the interactions are turned on, each charge fluctuation mode in the continuum experiences a scattering phase shift  $\delta(\vec{q}, \nu)$  which has the effect of changing the density of states of charge fluctuations. The zero-point energy describes the change in the energy of the continuum due to these scattering effects.

## Exercises

**Exercise 7.1** Section 7.4.1 argued that, in an electron plasma with a neutralizing positive charge background (jellium), the Hartree contribution to the ground-state energy is eliminated, so that the leading-order expression for the ground-state energy is

$$\frac{E_g}{V} = (2S+1) \int_{\mathbf{k}} \frac{\hbar^2 k^2}{2m} f_{\mathbf{k}} - \frac{(2S+1)}{2} \int_{\mathbf{k}, \mathbf{k}'} f_{\mathbf{k}} f_{\mathbf{k}'} \frac{e^2}{\epsilon_0 (\mathbf{k} - \mathbf{k}')^2}. \quad (7.264)$$